Parametric analysis of a solar Organic Rankine Cycle trigeneration system for residential applications

Luca Cioccolanti
Università Telematica e-Campus,
Via Isimbardi 10, 22060 - Novedrate, CO, Italy.
Email: luca.cioccolanti@uniecampus.it;

Roberto Tascioni
Università degli Studi Guglielmo Marconi
Via Plinio 44, 00193 - Roma, Italy
Email: r.tascioni@lab.unimarconi.it;

Enrico Bocci
Università degli Studi Guglielmo Marconi
Via Plinio 44, 00193 - Roma, Italy
Email: e.bocci@unimarconi.it

Mauro Villarini*
Tuscia University of Viterbo
Via San Camillo de Lellis, snc , 01100 – Viterbo, Italy
Email: mauro.villarini@unitus.it

Abstract

In this paper, the potential of a small scale concentrated solar Organic Rankine Cycle unit coupled with an absorption chiller for trigeneration purposes is investigated using a simulation analysis.
At the moment, only few research works encompass small-scale solar trigeneration systems and most of them do not refer to real plant. On the contrary, in this work electric, heating and cooling maximum generation of a real and experimental small scale prototype system composed of a 50 m^2 CPC solar field, a 3.5 kWe ORC plant and a 17 kWc absorption chiller is investigated by means of TRNSYS. In particular, this work relies on the evaluation of the dynamic performance of the mentioned plant varying some selected system parameters to provide proper modifications of its design configuration and operation.
More precisely, working temperature ranges, heating and intermediate fluid flow rates as well as volume of the storage tanks and size of the solar field have been varied within the simulation model. Results have shown that operating temperature ranges of the storage tanks considerably affect the overall performance of the system; by appropriately choosing these ranges the primary energy production can be increased by 6.5% compared to the baseline configuration without any additional investment costs. Moreover, setting suitably some design parameters can significantly contribute to extend the operating hours and the feasibility of a such small scale integrated system for residential applications.

Keywords: simulation analysis; concentrated parabolic compound solar collector; small-scale ORC; absorption chiller; renewable energy production; combined cooling heating and power.

Nomenclature

A	area of the collector [m^2]
a_0	first order efficiency coefficient [W/m^2·K]
a_1	second order efficiency coefficient [W/m^2·K]
CCHP	Combined Cooling, Heating and Power
COP	Coefficient Of Performance
CPC	Compound Parabolic Collector
DNI	Direct Normal Irradiation [W/m^2]
FESR	Fuel Energy Saving Ratio
G_b	direct radiation on collector plane [W/m^2]
G_d	diffuse radiation on collector plane [W/m^2]
h_{abs}	operating hours of the absorption chiller [h]
h_{ORC}	operating hours of the ORC unit [h]
HTT	High Temperature storage Tank
LTT	Low Temperature storage Tank
K_θ	Incident Angle Modifier for direct radiation
K_d	Incident Angle Modifier for diffuse radiation
NTU	Number of Transfer Units
P_e	Electrical Power [kWe]
P_c	Cooling Power [kWc]
P_t	Thermal Power [kWt]
SM	Solar Multiple
TES	Thermal Energy Storage
T_a	ambient air temperature [°C]
T_{av}	average temperature [°C]
T_m	mean temperature of the fluid in the collector [°C]
PEP	Primary Energy Production [kWh]
$\dot{m}_f$	mass flow rate of the organic fluid [kg/s]
Δh_e	actual specific enthalpy difference across the expander [kJ/(kg K)]
Δh_p	actual specific enthalpy difference across the pump [kJ/(kg K)]
ΔT_h	hot period working temperature range of HTT-ORC inlet [°C]
ΔT_c	cold period working temperature range of HTT-ORC inlet [°C]
ΔT_m	mid seasons working temperature range of HTT-ORC inlet [°C]

Greek symbols

β	absorptance coefficient
ε	emittance coefficient
η_{el}	electrical efficiency
$\eta_{e,ORC}$	ORC unit electrical efficiency
η_m	meccanical efficiency
η_o	maximum optical efficiency
$\eta_{t,ORC}$	ORC unit thermal efficiency
$\eta_{glob,CCHP}$	CCHP global efficiency

1. Introduction

One of the major concerns threatening our society is the world increasing energy demand. Fossil fuels are limited and the related environmental impact has serious effects on human health, ecosystems and climate. Therefore, in the last decades renewable energy technologies such as PVs and wind turbines have been widely adopted and energy production from renewables has accounted for about 19.2% of the global final energy consumptions in 2014 [1].

Among renewable energy technologies, solar technologies are becoming more and more attractive thanks to their increasing cost-competitiveness. Also, the industrial capacity of Concentrated Solar Power (CSP) is increasing especially in developing countries. CSP, indeed, is recognized as a

valuable alternative to substitute power generation from fossil-fueled plants due to its lower environmental impact [2]. Thanks to optical devices like lenses or mirrors the CSP technology is able to concentrate sunlight from a large area onto a small one and to convert it into electrical or thermal power depending on the applications. With respect to the method of capturing solar thermal energy, four main CSP technologies are available at present: Parabolic Trough Collector (PTC), Solar Power Tower (SPT), Linear Fresnel Reflector (LFR) and Parabolic Dish System (PDS) [3]. Compound Parabolic Collector (CPC) is also another suitable option due to its low cost and good thermal performance for low and medium temperature ranges [4]. It is able to collect both direct and diffuse solar radiation without a tracking system. One of its very promising applications is in combination with Organic Rankine Cycles (ORC) as already addressed by several studies [5,6]. For example, Antonelli et al. [7] already investigated the integration of small size compound parabolic collectors with ORC for electricity distributed production using the simulation tool AMESim.
An Organic Rankine Cycle plant works similarly to a Rankine steam power plant but it makes use of organic working fluids which fit low grade heat not incurring issues of water use at low temperatures presenting the advantages mentioned in [8]. Therefore, for low grade heat organic Rankine fluids perform better than water. Moreover, such system exhibits great flexibility, high safety and low maintenance requirements in recovering low temperature heat even at small scale [9]. Recently, many researchers are focusing on this field: Li et al. [10], for example, evaluated the influence of heat source temperature and ORC pump speed on the performance of a small-scale ORC system using R245fa as working fluid. Al Jubori et al. [11] instead focused on the influence of several turbine design features on turbine performance in ORC systems with five working fluids. Pei et al. [12] experimentally investigated the performance of a specially designed radial-axial turbine using R123 as working fluid. The test has shown that a turbine isentropic efficiency of 65% and an ORC efficiency of 6.8% can be obtained with a temperature difference of about 70°C between the hot and the cold sides. The same authors [13] evaluated the energetic and exergetic performance of the updated ORC system and the related thermal efficiency at different heat source temperatures. On the contrary, Quoilin et al.[14] evaluated the thermodynamic performance of low cost solar organic Rankine cycles considering different working fluids, expansion machines and system configurations.
However, in order to achieve higher conversion efficiencies and annual performance of ORC systems even at small scale the modeling of the different subsystem and their integration are of fundamental importance. For example, He et.al [15] developed a transient simulation model of a typical PTC system coupled with an ORC focusing on the effects of several key parameters. In particular, the authors evaluated the incidence of different size of the thermal storage tank on the performance of the system with seasonality. Instead, Borunda et al [16] evaluated the potential of PTC-ORC system as cogeneration unit in a textile industrial process using TRNSYS to emulate the real operating conditions of the user. Furthermore, very important, as a reference for the present study, is the contribution of Calise et al. [17] who developed a dynamic simulation model of a 6 kWe ORC coupled with 73.5 m^2 of innovative flat-plate evacuated solar collectors whose heat input to the evaporator is integrated by an auxiliary heater fed with natural gas. Authors performed also a sensitivity analysis to evaluate the combination of different design parameters which maximize the thermo-economic performance of the system. This work, even though examining a CHP, differently than our CCHP configuration, allows an effective comparison with our system.
In general, micro cogeneration and trigeneration have a very interesting potential in households [18] both grid connected and stand alone and several studies have addressed the dynamic performance of such systems in TRNSYS [19,20]. For example, Angrisani et al. [21] investigated the techno-

economic feasibility of a micro-trigeneration system starting from previous experimental tests of the prime mover. The integrated system used to provide air conditioning to a lecture room and domestic hot water to a nearby household has shown interesting performance, synthesized by an 82.1% overall efficiency in terms of primary energy ratio, and reduced energy consumptions compared to the reference system. They specifically developed a mathematical model of a micro-trigeneration system with the final aim to determine the primary energy saving by means of the Fuel Energy Saving Ratio (FESR). They implemented also a sensitivity analysis of primary energy saving, net saving and CHP generation bonus with respect to the electric surplus factor from the CCHP unit. However, attention has not been paid on the influence of design and adjustment parameters on plant performance. Considering the works edited until now on the topic of solar ORC as Combined Cooling Heating and Power (CCHP) system, Chang et al. [22] referred to a CCHP system consisting of a hybrid Proton Exchange Membrane fuel cell and a solar ORC. In particular, they evaluated the effects of solar radiation, current density and operating temperature of the fuel cell and ambient temperature on the performance of the trigeneration system. However, in this study the electric power is provided only by the fuel cell thus mitigating the energy dependence on the solar source because the solar powered ORC expander is coupled with the vapor compressor cycle compressor. Boyaghchi et al. [23], instead, carried out a thermodynamic and thermoeconomic optimization of a solar ORC trigeneration plant for domestic applications by varying some thermodynamic variables. The heat coming from solar collectors is integrated by a natural gas boiler when requested. They focused the attention on the following CCHP key parameters: turbine inlet temperature and pressure, turbine back pressure, evaporator temperature and heater outlet temperature. The considered objective functions were the thermal efficiency, the exergy efficiency and the total product cost rate.

In this paper an integrated pilot system installed near Orte [24,25] is considered. The main novelty of this work relies on the assessment of the influence of some operating and design parameters on the performance of the system. The final aim of this work is to provide useful information on the best operating conditions of the prototype plant in order to increase its overall energy production. Therefore, the present work focuses the attention, for the first time, on a CCHP integrally powered by solar radiation and, furthermore, gives an added value to the existing literature on solar ORC CCHP especially with respect of the selection of the system design and optimal operation parameters. Hence, the paper is organized as follows: after the Introduction, Section 2 describes the whole prototype plant; Section 3 reports a short description of the numerical model while Section 4 describes the parametric analysis in detail; Section 5 presents and discusses the main results of the work and Section 6 reports the conclusions.

2. Plant description

The integrated prototype plant under analysis consists of: (i) a 35 kWt CPC solar plant composed of solar collectors developed and patented by K-Engineering and Kloben Sud [26]; (ii) a 3.5 kWe regenerative Organic Rankine Cycle unit produced by Newcomen [27]; (iii) a 17 kWc absorption chiller by Yazaki Energy Systems [28]. Other components of the system are also the evaporative cooling tower to dispose the heat from the absorption chiller and two 3 m^3 heat storage tanks. The heat-carrying fluids used within the High Temperature Tank (HTT) and the Low Temperature Tank (LTT) are respectively diathermic oil and water. Considering the size of solar field and ORC, the HTT has the role to recover the heat from the solar field when it would not be enough to run the ORC. In the same way, the LTT allows to extend the operation of the absorption chiller when the ORC unit is off. Therefore, the HTT decouples the thermal energy production by the solar field and the energy supply to the ORC; while the LTT decouples the ORC thermal output and the absorption chiller. Since the ORC and the absorption chiller need the inlet temperature of the heating fluid within a certain range, the above-mentioned TES tanks are used to allow electric, refrigerating and thermal powers generation apart from instantaneous solar radiation extending in the time the overall system energy production.

The solar plant is able to reach heat fluid temperatures up to 190°C by means of copper tubes for high vacuum applications. The absorbing surface consists of a Al–N/Al selective material with an absorptance coefficient $\beta>0.92$ and an emittance coefficient $\varepsilon<0.065$. Two fluid loops separate the collected heat from the solar plant to the ORC unit using therminol 62 as thermal vector thanks to its high thermal stability up to 325°C and low vapor pressure [29]. As regards the ORC unit, the expander is a three radial cylinders alternative engine and it comes with R134a as working fluid. However, because of the absorption chiller that requires higher temperatures and in order to increase the electrical conversion efficiency, R245fa has been considered in our analysis. Indeed, temperatures pertinent to R134a would have not permitted to feed the absorption chiller at the requested temperature after the expansion within the ORC unit. Moreover, R245fa has low specific volume ratio, high molecular weight, zero Ozone Depletion Potential, it is inexpensive, non-corrosive and non-flammable. Finally, its critical temperature is above the ORC maximum operating temperature which is in the range 100-150°C depending on seasonality. Therefore, all these characteristics make it suitable for the considered application.

The released heat by the ORC unit flows to the LTT which in turn feeds the heating and cooling loads. In the latter case, the fluid released its heat to the absorption chiller which in turn provides cold water at a nominal temperature of 7°C. In terms of performance, the absorption chiller has a nominal Coefficient Of Performance (COP) of 0.7 with 88°C inlet hot water temperature and 7°C chilled water output temperature. Moreover, it is able to work with acceptable performance up to 70°C with a 12.5 kW refrigerating power instead of the 17.6 kW nominal power.

Hence, the temperature at the condenser have been fixed to satisfy the related heating and cooling needs with radiant panel floors where the lowest heating temperature is set to 30°C and the highest cooling temperature to 15°C. Table 1 reports the characteristics of the main plant components while Figures 1 show some of them.

Table 1 - characteristics of the main components and operating conditions

Design specifications	Value	Producer	Operating conditions	Value
Solar Collectors Area	50 m^2	Kloben	ΔT_h	180-160 °C
ORC System	3 kWe	Newcomen	ΔT_c	130-110 °C
Absorption chiller	17.6 kWc	Yazaki	ΔT_m	160-135 °C
Pumps	30-120 l/min; 10 m*	Wilo	CPC-HTT mass flow rate	7000 kg/h
HT Storage Tanks	3 m^3 ; 4W/K**	Kloben	HTT-ORC mass flow rate	1800 kg/h
LT Storage Tanks	3 m^3 ; 4W/K**	Kloben	LTT_abs-2 mass flow rate	3600 kg/h
Temperature @Terminals	Winter: 30°C Summer:15°C		LTT_abs mass flow rate	4320 kg/h
Site	Orte (Italy)		Local coordinates	42° 45' 74.41'' N 12° 38' 69.84'' E

*pressure head

**heat losses

Figure 1 - (a) the solar collector; (b) the ORC unit; (c) the absorption chiller

Moreover, to complete the outline of the solar CCHP system, a breakdown of the costs, incurred in the STS research project [25], has been reported in Table 2 showing that the complexity of the system compared to traditional solar technologies entails higher investment cost. However, since it is a prototype unit, it is reasonable to expect lower cost in case of large scale industrial production.

Table 2 –Breakdown of the costs of the trigeneration system

Component	Quantity	Unit cost	Total cost
4.15 m^2 each solar collector	12	€ 1,250 [26]	€ 15,000
3 kWe ORC System	1	€ 15,000 [27]	€ 15,000
17.6 kWc Absorption chiller*	1	€ 22,500 [28]	€ 22,500
Pumps	4	€ 700 [30]	€ 2,800
3 m^3 HT and LT Storage Tanks	2	€ 1,500 [26]	€ 3,000
System component fitting **	lump sum		€ 15,000 [30]
Total sum			**€ 73,300**

* included the evaporative cooling tower

** included 200 m piping, heat exchangers and plant control system

By the way, costs of Calise et al. [17] showed the following expense item within their capital costs analysis: a 25,725 € cost of the solar collectors corresponding to 350 €/m^2 (to be compared with our 301 €/m^2); 35,000 € as cost of the 6 kW ORC unit corresponding with 5,833 €/kWel (to be compared with our 4,000 €/kWel) and 7,717 € regarding valves, fittings, pipes, etc. The incidence of this cost category in the breakdown presented in table 2 is much higher (100% of the overall solar collectors capital cost) because it represents the engineering, the piping, the system adjustment and the pertinent automatic valves and sensors of a prototype and with an evaporative tower and an absorption chiller. The final different cost between the two systems is represented by the 11.4 €/W_e [17] compared with the 24.4 €/W_e of the present system which will result a decisive factor.

3. Model description and validation

Starting from the prototype plant installed near the city of Orte in Italy, a dynamic simulation model of the whole system has been developed in TRNSYS [31], a well-known software diffusely adopted for both commercial and academic purposes. This software tool allows to include in the model also the fluctuant and variable radiation of the sun with regards to the site of location of the plant and to analyze and monitor the behavior of the integrated system. There are many references in literature [6,16–21,24] showing the effectiveness of its application for the simulation of solar powered ORC plants which make use of the library built-in components and ad hoc subroutines developed by the users.

Although TRNSYS library has a wide range of tested types for the simulation of many components, in this work a specific subroutine for the ORC unit has been customized by the authors in Matlab [32]. More precisely, the main components of the model are: Type 71 for the CPC solar field; Type 4 for both the diathermic oil tank (HTT) and the hot water storage tank (LTT), Type 155 for calling Matlab, Type 107 for the absorption chiller and Type 510 for the evaporative cooling tower. Weather data in terms of solar radiation and ambient temperature have been taken from Meteonorm database on an hourly basis. Since the scope of the paper is to analyse how the performance of the system are affected by the variation of the operating and design parameters independently from the specific energy demand, the final user thermal demand is simply represented by three Type 4 (load, load-2 and load-3) with very large capacity to potentially collect the whole heating, cooling and hot water energy production as reported in Figure 2.

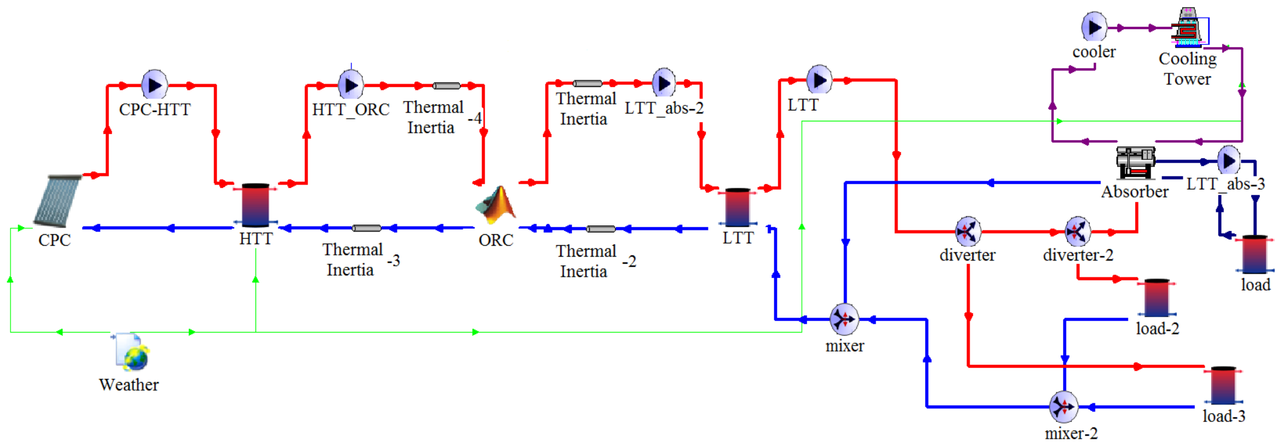

Fig. 2 - Scheme of the simulation model

With reference to the different subsystems, the following assumptions have been considered for the ORC unit according to the specifications of the manufacturer:

- no pressure drops across the components;
- no thermal capacity of the components;
- thermal losses in the storage tanks only;
- minimum driving temperature difference between the evaporator and the condenser and pressure ratio at the expander equal to 50°C and 2.5;
- maximum inlet pressure at the expander 25 bar;
- constant isentropic efficiency of the pump (70%);
- expander isentropic efficiency varying in the range 46-60%;
- constant efficiency of the heat exchangers;
- steady state conditions.

In addition, an electrical efficiency of 90% both for the pump electric motor and the expander generator and a mechanical efficiency of 95% have been assumed. The heat transfer rate in the heat exchangers is assessed by means of the Number of Transfer Units (NTU) method.

The R245fa flow rate varies with ambient conditions and is calculated according to an iterative procedure developed in Matlab fixing a 5°C overheating and a 149°C maximum evaporation temperature. Conditions of inlet oil and water at the evaporator and condenser respectively are taken from TRNSYS while those of organic working fluid are initialized in Matlab. Then, the temperature difference at the evaporator, the working fluid flow rate and the related thermodynamic states are assessed according to an iterative procedure as schematically shown in Figure 3. In particular, a minimum temperature difference of 34°C between the inlet diathermic oil temperature and the evaporating temperature has been fixed while the pinch point at the evaporator varied accordingly.

Finally, R134a and R245fa has been considered as working fluid and the values of its thermodynamics properties based on the open source library Coolprop [33].

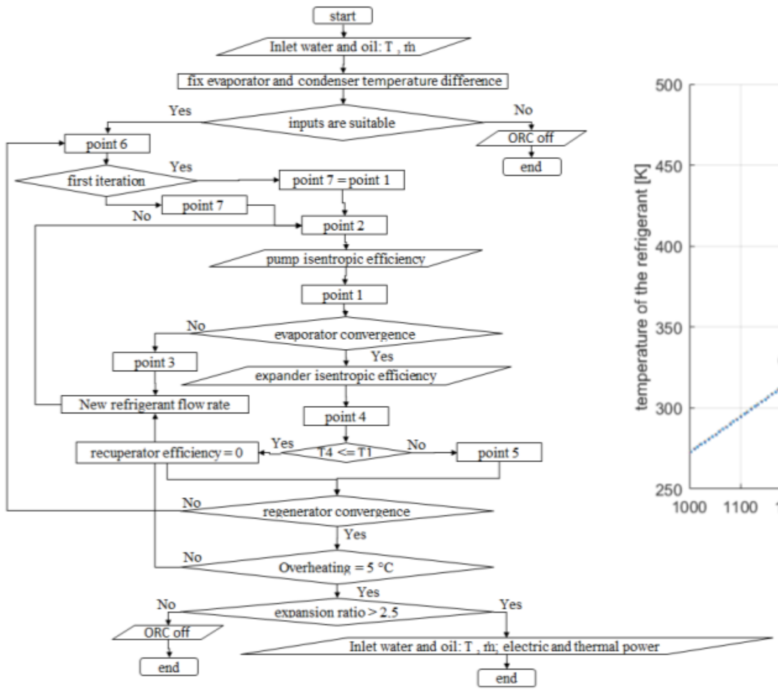

Fig. 3 – Diagram of the logic of the ORC model

At very low-part load conditions, the ORC power output is similar to the absorbed power by the auxiliaries. Therefore, always regarding R245fa, a minimum 50°C temperature difference between the heat source and the sink has been assumed to run the ORC unit conveniently. In order to reduce the thermal losses in the HTT storage tank, the diathermic oil flows from the CPC solar field to the HTT storage tank if its outlet temperature is at least 5°C higher than the average temperature of the tank (T_{av}). The HTT_ORC and LTT_abs-2 pumps, shown in Figure 2, are turned on as soon as the average temperature of the HTT storage tank is > 130°C while they are switched off when this temperature decreases to less than 110°C. Accordingly to the power available at the solar field, flow rates of these pumps have been fixed equal to 1800 kg/h and 3600 kg/h respectively. As regards the LTT_abs pump, it operates with a nominal water flow rate of 4320 kg/h at temperatures ranging from 28-33°C in the cold period, 50-55°C in the mid seasons and 70-75°C in the hot period to supply adequate thermal power to the absorption chiller. The heating demand is considered only in the cold period 1 November -15 April according to the Italian decree 412/93 [34] which has fixed the heating period for the different locations in Italy. On the contrary, the hot period has been assumed as 1 June - 30 September when the maximum daily mean temperature of Rome (near Orte) is greater than 26°C and cooling demand is requested. Finally, in the remaining period of the year approximately corresponding to the mid seasons, the energy from the LTT is used to satisfy the domestic hot water demand. Therefore, the operation of the mixers and the diverters as reported in Figure 2 depends on seasonality. In particular, the diverter-2 redirects the flow to the load-2 in the mid seasons for hot water production or directly to the absorption chiller in the hot season for cooling purposes. Finally, an evaporative cooling tower extracts heat when the absorption chiller is in operation by means of a constant flow rate of about 9180 kg/h according to the specifications of the chiller.

In terms of performance, the useful power, Pu, from the solar field is equal to Eq.1:

$$P_u = A \cdot (\eta_0 \cdot (G_b \cdot K_\theta + G_d \cdot K_d) - a_0 \cdot (T_m - T_a) - a_1 \cdot (T_m - T_a)^2) \quad (1)$$

where A is the collector area, G_b and G_d the direct and diffuse radiation on collector plane, K_θ and K_d the Incident Angle Modifier for direct and diffuse radiation respectively, T_m the mean temperature of the fluid in the collector obtained as $(T_{inlet}+T_{outlet})/2$ according to an iterative procedure, T_a the ambient air temperature and η_0 the maximum optical efficiency. Finally, a_0 and a_1 are coefficients which depend on the type and model of the collectors considered equal to 0.974 and 0.005 W/m^2·K respectively in this case.

With reference to the ORC unit, the electric power produced is:

$$P_{el} = \dot{m}_f \cdot [\eta_m \cdot \eta_{el} \cdot \Delta h_e - \Delta h_p/(\eta_m \cdot \eta_{el})] \quad (2)$$

with $\dot{m}_f$ the organic fluid flow rate, η_m the mechanical efficiency, η_{el} the electrical efficiency, Δh_e and Δh_p the actual specific enthalpy difference across the expander and the pump. Finally, the cooling power of the absorption chiller is equal to Eq. 3:

$$P_c = P_t \cdot COP \quad (3)$$

where P_t is the inlet thermal power and COP depends on the operating conditions.

Besides the generated power, the performance of the integrated plant have been evaluated also in terms of conversion efficiencies, operating hours and energies as reported in Section 5.

The ORC model discussed above has been validated using R134fa as working fluid on the basis of the experimental results presented by Bianchi et al. [33, 34] who presented three different sets of experimental data using the same Newcomen ORC unit. The Table 3 shows that the model proved (whose heading of column indicated as “M”) to be in good agreement with the experimental results (whose heading of column indicated as “E”) with an error band in the range ±5%.

Table 3 – Comparison between experimental and model data

	E1	M1	Error	E2	M2	Error	E3	M3	Error
T3 [°C]	64.6	63.9	1.1%	73.8	73.8	0.0%	86	88.8	-3.3%
T4 [°C]	41.7	40.11	3.8%	51.2	51.38	-0.4%	63.8	67.2	-5.3%
T7 [°C]	34.5	32.5	5.8%	40.35	38.2	5.3%	47.9	47	1.9%
T6 [°C]	23	22.65	1.5%	22.9	22.65	1.1%	23.1	22	4.8%
$\dot{m}_f$ [kg/s]	0.1	0.1	0.0%	0.1	0.1	0.0%	0.09	0.09	0.0%
$\eta_{e,ORC}$	3.67	**3.79**	-3.3%	3.98	**4.06**	-2.0%	4.2	**4.28**	-1.9%
P2 [°C]	14.3	14.5	-1.4%	14.3	14.5	-1.4%	14.3	14.4	-0.7%
P6 [°C]	6	6.07	-1.2%	6	6.08	-1.3%	6	6.08	-1.3%

In addition, the experimental findings have shown that the working temperature is the most critical parameter, indeed the table 3 confirms the slight raise in electric efficiency with varying the maximum operating temperature of the organic fluid. The operating temperature has an opposite effect on the solar collector and on the ORC unit: higher the temperature of the fluid lower the solar panel efficiency because of the thermal losses; on the contrary the ORC efficiency increases with temperature because of the higher temperature difference. Besides, the operating temperature depends on the working temperature set point, the volume of the solar tanks and the mass flow rates of the fluids. Therefore, a parametric analysis has been carried out in order to evaluate the effect of these different parameters on the overall plant performance.

4. Parametric analysis

Initially, the performance of the system have been evaluated at the design conditions (configuration C1) mentioned above and reported in Table 1.
After that, influence of several key parameters has been investigated in order to assess the more efficient operating and design configuration of the system.
More precisely, the following parameters have been varied:

- the working temperature ranges of the HTT storage which is a very relevant parameter. When the temperature at the HTT storage tank reaches the higher temperature of the mentioned range, the ORC switches on while when it goes down below the lower value of the range, the ORC switches off;
- the mass flow rate of the fluids in the loops;
- the solar multiple (SM) which is the ratio between the power capacity of the solar field and the design power expected from the solar field to assure the ORC operation at nominal conditions. For the same location, the SM depends on the square meters of the solar collectors installed;

- the inertia of the system in terms of HTT and LTT storage tank and pertinent fluid flow rates considering that the mass flow rate is requested to vary accordingly to the volumes of thermal storage tanks [15];
- the DNI of the site.

Once the temperatures at the condenser have been fixed with seasonality, the operating temperatures of the CPC-ORC loop depend on the maximum allowable temperature of the considered CPC solar field and the expansion ratio of the expander. Besides the baseline temperature range, two different operating conditions have been considered: the extended temperature range (as for configuration C2) and the reduced temperature range (as for configuration C3). In particular, the working temperature ranges of the CPC-ORC loop have been varied according to Table 4.

Table 4 - Working temperature ranges of the HTT-ORC inlet

Temperature range	ΔT_h	ΔT_c	ΔT_m
Baseline	180-160 °C	130-110 °C	160-135 °C
Extended	190-160 °C	140-110 °C	160-135 °C
Reduced	170-160 °C	120-110 °C	160-135 °C

With respect to the mass flow rate in the different loops, it has been increased by 50% (configurations C4 for reduced temperature range and C5 for extended temperature range) and reduced of 50% (configurations C6 for reduced temperature range and C7 for extended temperature range) compared to the baseline. As regards the design conditions, the SM has been increased by 50% (configurations C8 and C9 for reduced and extended temperature range respectively) and by 100% (configurations C10 and C11 for reduced and extended temperature range respectively) compared to the prototype plant. Inertia of the system has been changed compared to the baseline by increasing the flow rate of the pumps and the volume of the HTT and STT of 50% and 1 m^3 in case of increased inertia (configurations C12 for reduced temperature range and C13 for extended temperature range) and vice versa in case of reduced inertia (configurations C14 and C15 for reduced and extended temperature range). Finally, with respect to the influence of the DNI the plant performance have been evaluated also for the city of Palermo in Italy (local coordinates: 38° 11’ 56.88’’ N and 13° 36’ 12.67’’ E) considering a SM equal to 2 and a reduced temperature range (configuration C16). Table 5 summarizes the values of the key parameters for the different simulations:

Table 5 - Range of the key parameters for the different configurations

Configuration	ΔT_h [°C]	ΔT_c [°C]	ΔT_m [°C]	SM (Collectors Area, [m^2])	CPC-HTT [kg/h]	HTT-ORC [kg/h]	LTT_abs-2 [kg/h]	LTT_abs [kg/h]	HTT [m^3]	LTT [m^3]
C1	180-160	130-110	160-135	1 (50)	7000	1800	3600	4320	3	3
C2	190-160	140-110	160-135	1 (50)	7000	1800	3600	4320	3	3
C3	170-160	120-110	160-135	1 (50)	7000	1800	3600	4320	3	3
C4	170-160	120-110	160-135	1 (50)	10500	2700	5400	6480	3	3
C5	190-160	140-110	160-135	1 (50)	10500	2700	5400	6480	3	3
C6	170-160	120-110	160-135	1 (50)	3500	900	1800	2160	3	3
C7	190-160	140-110	160-135	1 (50)	3500	900	1800	2160	3	3
C8	170-160	120-110	160-135	1.5 (75)	7000	1800	3600	4320	3	3

C9	190-160	140-110	160-135	1.5 (75)	7000	1800	3600	4320	3	3
C10	170-160	120-110	160-135	2 (100)	7000	1800	3600	4320	3	3
C11	190-160	140-110	160-135	2 (100)	7000	1800	3600	4320	3	3
C12	170-160	120-110	160-135	1 (50)	10500	2700	5400	6480	4	4
C13	190-160	140-110	160-135	1 (50)	10500	2700	5400	6480	4	4
C14	170-160	120-110	160-135	1 (50)	3500	900	1800	2160	2	2
C15	190-160	140-110	160-135	1 (50)	3500	900	1800	2160	2	2
C16	170-160	120-110	160-135	2 (100)	7000	1800	3600	4320	3	3

5. Results and discussion

In general, the performance of the system has been evaluated in terms of operating hours, electric, thermal and conversion efficiencies and energy production. Table 6 reports the performance of the integrated system under conditions of configuration C1 according to a monthly basis.

Table 6 - Monthly performance of the system for configuration C1

	η_{CPC} [%]	$T_{av,HTT}$ [°C]	$T_{av,LTT}$ [°C]	h_{ORC}	$\eta_{e,ORC}$ [%]	$\eta_{t,ORC}$ [%]	COP_{abs}	h_{abs}
Jan	41.1	112.6	27.7	27.3	4.8	68.4	0.00	0.0
Feb	49.3	116.8	28.9	46.7	4.7	68.7	0.00	0.0
Mar	57.1	117.6	28.6	74.5	4.8	68.3	0.00	0.0
Apr	51.6	132.1	40.0	67.8	4.7	69.8	0.00	0.0
May	50.2	145.2	50.7	68.3	4.5	72.0	0.00	0.0
Jun	32.8	170.8	68.6	36.8	3.0	75.6	0.65	50.0
Jul	41.7	169.4	70.7	61.0	2.9	76.1	0.64	89.2
Aug	34.9	168.0	70.4	48.2	2.9	75.8	0.64	70.2
Sept	27.7	169.4	70.1	31.7	2.9	75.5	0.65	45.2
Oct	41.1	145.2	50.7	48.7	4.2	72.1	0.00	1.8
Nov	40.8	117.6	28.5	33.5	4.7	69.0	0.00	0.0
Dec	44.9	117.1	27.7	34.5	4.8	68.7	0.00	0.0

Although the higher average temperature of the HTT tank, the electric efficiency of the ORC ($\eta_{e,ORC}$) is lower in the hot season due to the higher temperatures at the condenser for cooling purpose. In particular, the monthly mean value of the ORC electric efficiency reaches 3.0 % during summer months and 4.8% during winter months. On the contrary, the thermal efficiency of the ORC ($\eta_{t,ORC}$) is kept higher than 68% throughout the year. Because of the limited area of the collectors, the operating hours of the ORC unit (h_{ORC}) are very limited in the cold season and the average temperature of the HTT tank ($T_{av,HTT}$) close to the minimum threshold. In the hot season the operating hours of the ORC increase whilst they reach a maximum during the mid season in May due to the lower condenser temperatures. The operating hours of the absorption chiller (h_{abs}) are limited to about 260 h since its operation is limited to the hot period while the COP is maintained almost constant at about 0.65.

For a given temperature at the condenser, the analysis of the results shows that the performance of the integrated system is largely affected by the temperature at the HTT storage tank. Therefore, the influence of different working temperature ranges of the CPC-ORC loop as in Table 3 has been analysed. In particular, with reduced temperature ranges the operating hours of the ORC unit during the hot season are substantially higher and they increase by more than 10% on a yearly basis (654 annual hours compared to 579 annual hours in C1). On the contrary, during the hot season the electric efficiency does not change because of the high temperature at the condenser and the high irradiation while the thermal efficiency increases with extended temperature range because of the higher average temperature at the HTT. Figures 4a-b show the trend of the monthly average electric and thermal efficiencies of the ORC unit while Figures 5a-b report the monthly energy production of the trigeneration plant for configurations C2 and C3 respectively compared to that of C1.

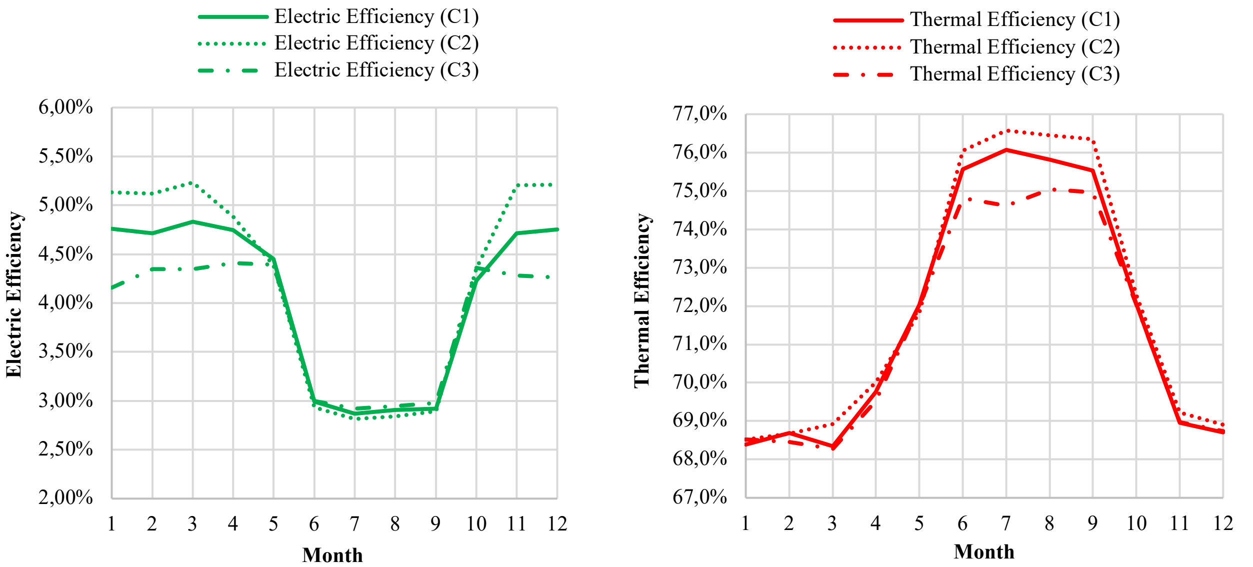

Figure 4 - Monthly average efficiencies of the ORC unit for different configurations, a) electric efficiency, b) thermal efficiency

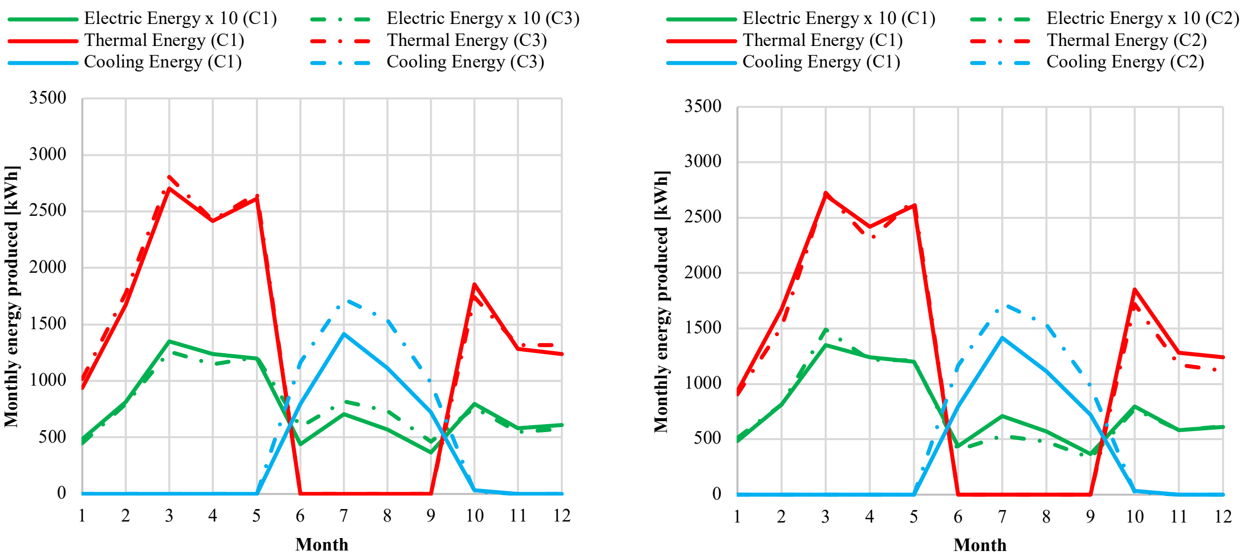

Figure 5 - Comparison of the monthly energy production of the trigeneration plant for different configurations, a) C1-C2, b) C1-C3

Besides the operating temperature ranges, the average temperature of the HTT storage tank and in turn the performance of the integrated system is affected also by the mass flow rate of the fluid in the different loops. Therefore, the influence of the fluids flow rate has been assessed considering a variation of ±50% with respect to the scenarios C2 and C3. In order to compare the system performance in the different scenarios also the equivalent Primary Energy Production (PEP) [37] is taken into account where the electric, heating and cooling energy productions are reported in terms of equivalent primary energy based on the Italian national thermoelectric efficiency [38] and a realistic value of COP equal to 3 of an equivalent vapour compression chiller [39]. In particular, results have shown that changes in the mass flow rate of the intermediate fluids (±50% with respect to those of the design configuration C1 as reported in Table 1) lower the overall PEP of the system independently from the operating temperature ranges of the HTT. This reduction is even greater at extended temperature ranges because of the lower conversion efficiency at the CPC and ORC operating hours in case of higher mass flow rates. The thermal energy production significantly reduces while the cooling energy production increases with respect to the reference mass flow rate of the fluid into the different loops. On the contrary, the electric energy production increases with a decrease of the mass flow rate of the fluids (C14 and C15) especially if compared with configuration with increase of the mass flow rate (C12 and C13) as shown in Table 7.

In general, in order to better evaluate the influence of the operating parameters such as the working temperature range of the HTT and the fluids mass flow rate the performance of the system have been evaluated also on a daily basis. Figures 6a-f show the daily trend of the main parameters for the three different periods of the year with respect to the best (C3) and the worst (C5) configuration in terms of PEP whose values are shown in Table 7.

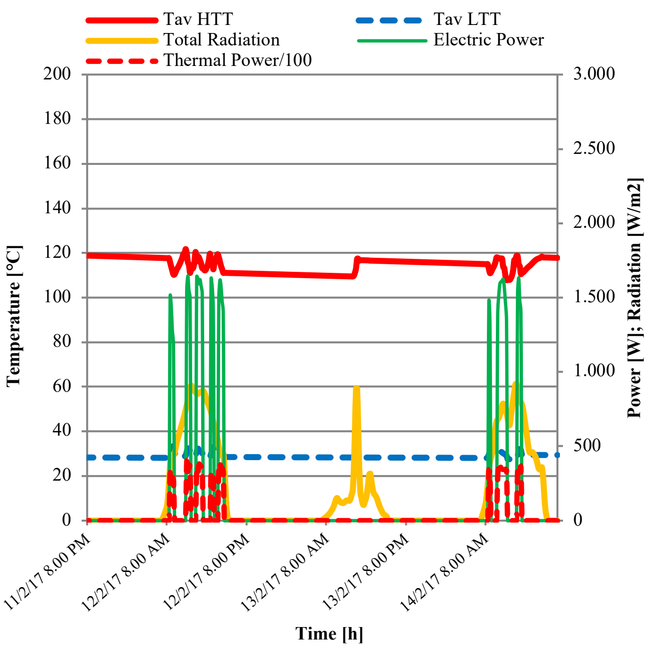

Figure 6-a

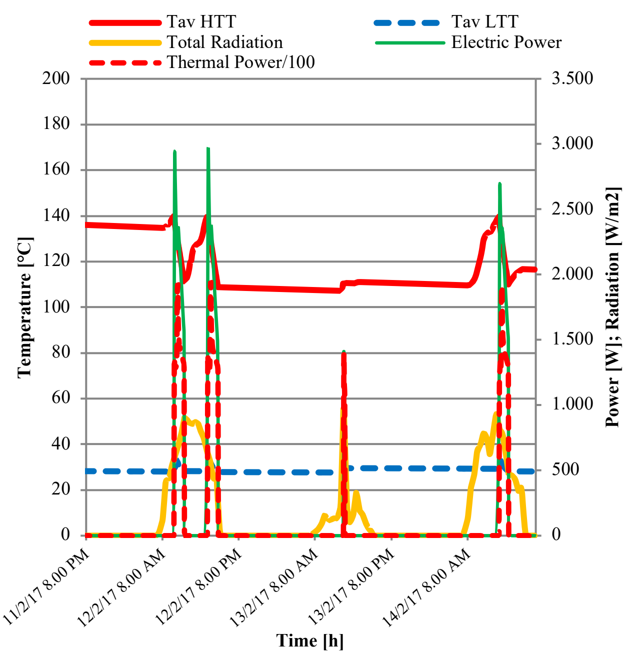

Figure 6-b

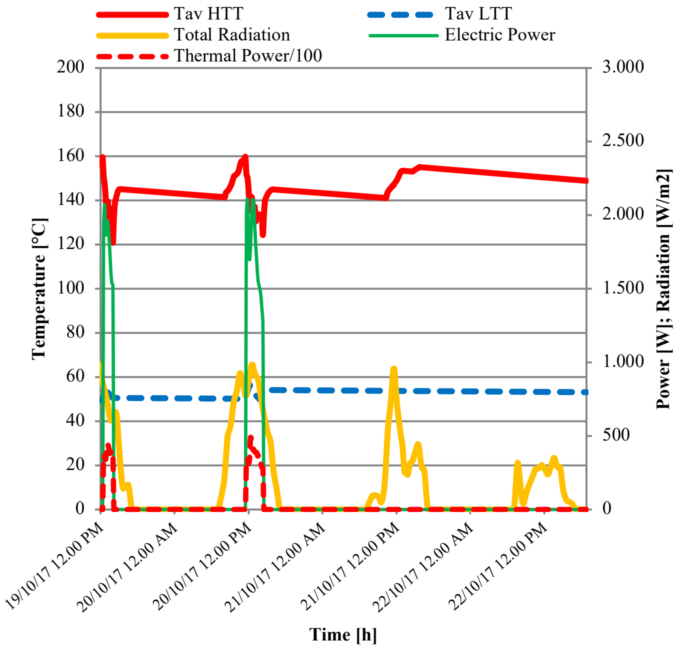

Figure 6-c

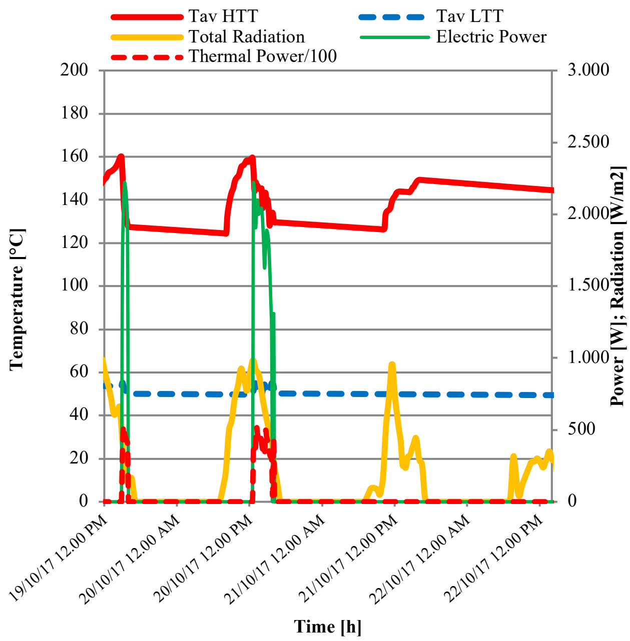

Figure 6-d

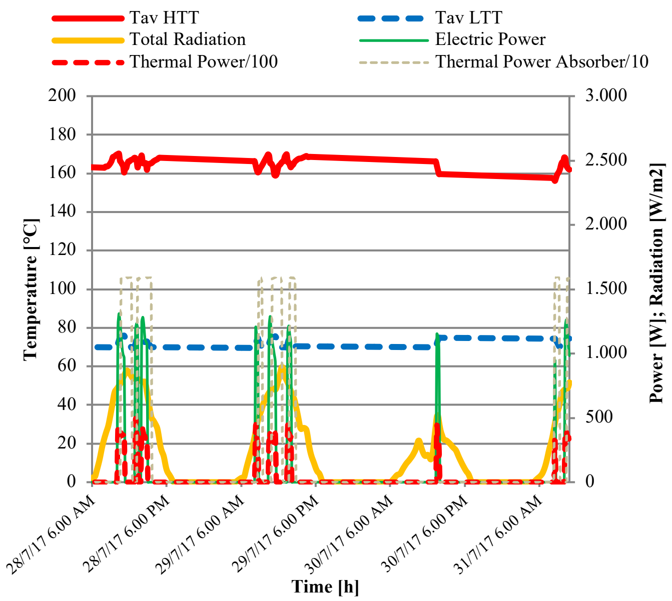

Figure 6-e

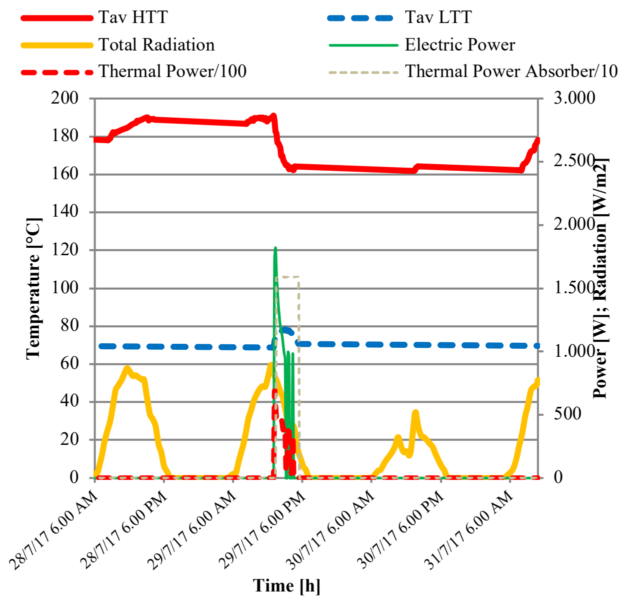

Figure 6-f

Figure 6 - Daily trend of the plant performance for configuration C3 and C5, during the cold season (a,b); mid season (c,d); hot season (e,f)

Compared to extended temperature ranges, reduced ones allow to increase the operation of the system during the year despite the higher number of shutdowns. The solar irradiation indeed is usually not sufficient to guarantee the prolonged operation of the ORC unit especially in the cold season. Therefore, in case of extended temperature ranges much more time is requested to heat up the HTT storage tank before the running of the ORC plant and the daily irradiation sometimes is not converted in useful power. For this reason, some design parameters such as the SM or the volume of the storage tanks have been varied and their influence on the overall performance of the integrated system assessed in order to evaluate rooms of improvement of the real system.

As regards the SM, higher the energy collected by the solar field higher the average temperature of the HTT tank and consequently the operation of the system. For this reason, the SM has been increased by 50% and 100% with respect to the design configuration. The performance of the system, with an increase of the SM by 50% and 100%, has been evaluated both at the reduced and extended temperature ranges. Independently from the SM the global performance of the system remain higher with reduced temperature ranges at the HTT storage tank because of the higher conversion efficiency at the CPC and operating hours of the ORC unit. Figures 7a-b and 8a-b show the monthly electric, thermal and cooling energy production of the integrated system with a SM equal to 1.5 and 2 respectively at different working temperature ranges of the HTT.

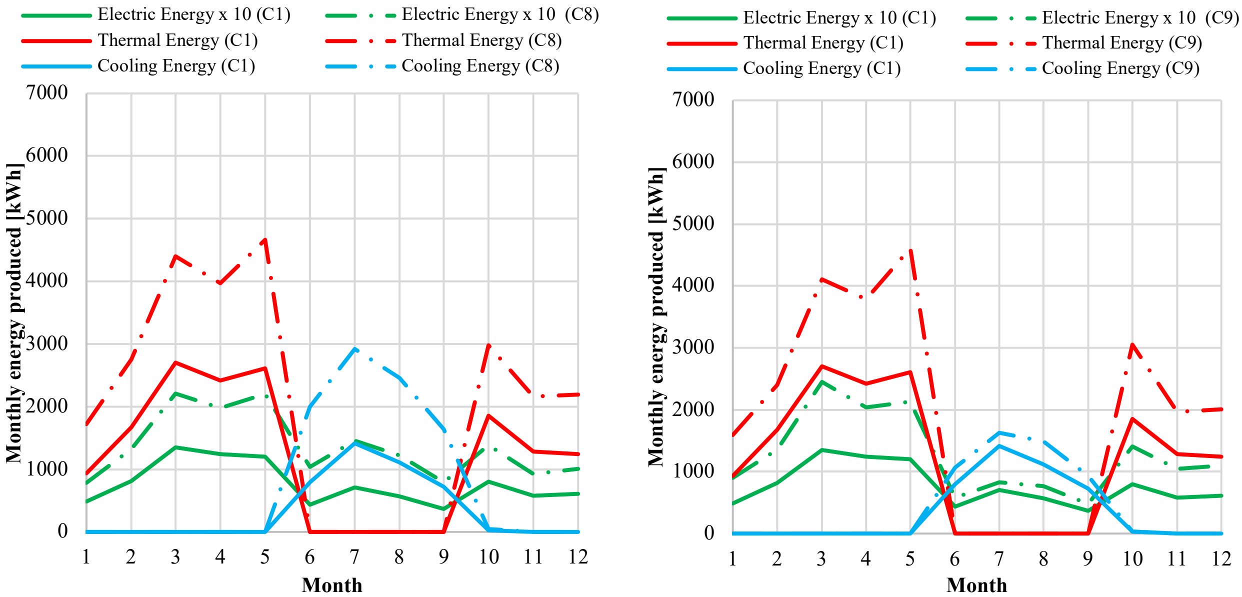

Fig. 7.a Fig. 7.b

Figure 7 - monthly energy production of the trigeneration plant with SM=1.5, a) reduced temperature ranges; b) extended temperature ranges

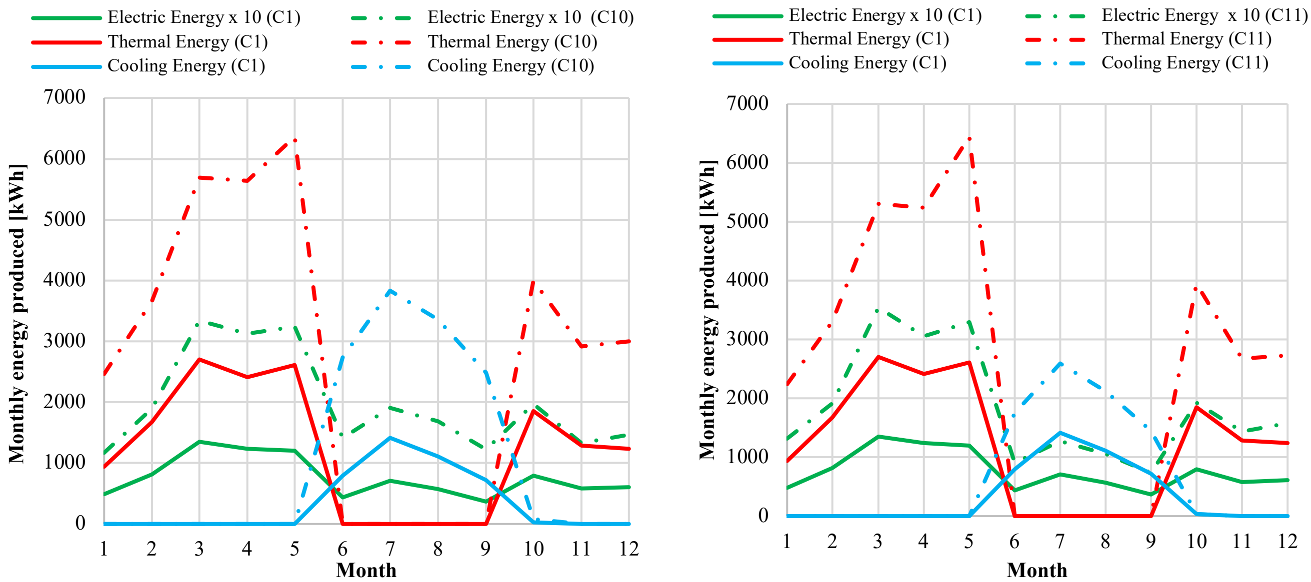

Fig. 8.a Fig. 8.b

Figure 8 - monthly energy production of the trigeneration plant with SM=2, a) reduced temperature ranges; b) extended temperature ranges

It can be noted that increasing the SM has a remarkable effect in terms of plant energy production. In general, reduced temperature ranges allow to substantially increase the performance of the system in the hot season while effects of the temperature ranges are limited during the cold and mid seasons. In terms of PEP, an increase of 50% of the SM allows to achieve an increase of about 65% compared to configurations C3 and C2 respectively as reported in the following Table 7. With a SM equal to 2 and reduced temperature ranges the annual operating hours of the plant more than double compared to configuration C3 and are about 2.5 higher than in configuration C1 reaching almost 1460 h which represents a very interesting target.

Volume of the HTT and LTT storage tanks has been varied as further parameter influencing the system storage capacity and inertia. The mass flow rate of the fluid in the loops of the system has been varied accordingly, as reported in Table 1. Figures 9a-d report the influence of these variations in terms of energy production of the plant.

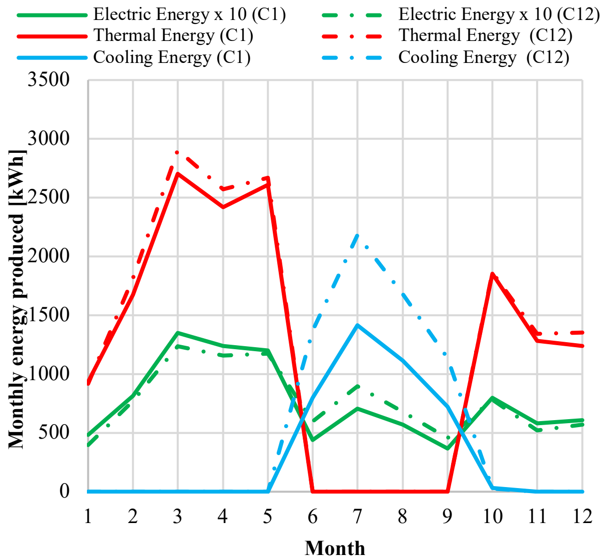

Fig. 9.a

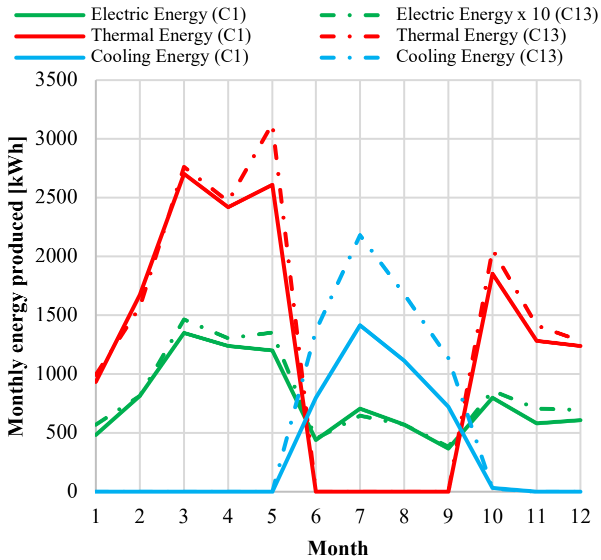

Fig. 9.b

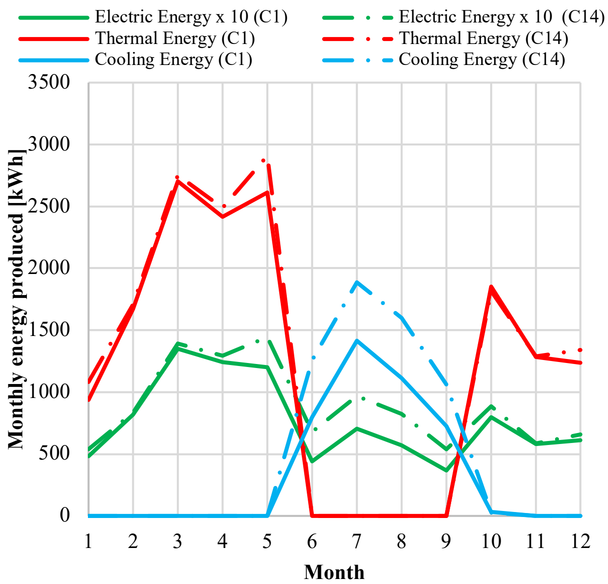

Fig. 9.c

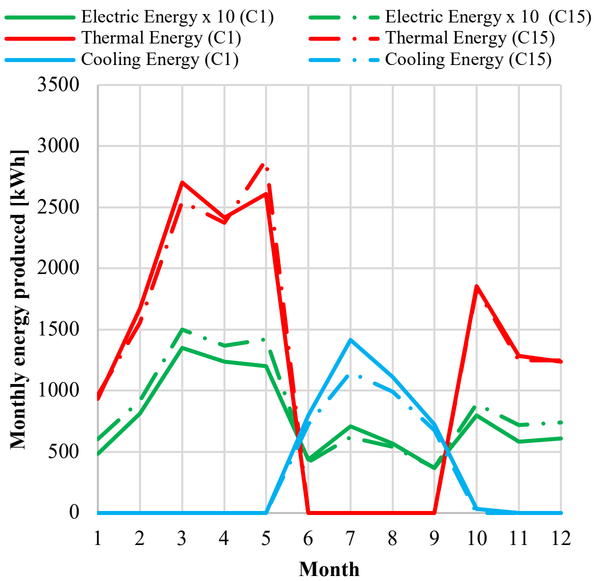

Fig. 9.d

Figure 9 - monthly energy production of the trigeneration plant varying inertia:

(a,b) increased inertia under reduced and extended temperature ranges;
(c,d) reduced inertia under reduced and extended temperature ranges

Changing the inertia of the system, by means of ±50% of the intermediate fluids flow rate and ±1 m^3 of the volume of the storage tanks with respect to the design configuration C1, slightly improves the overall performance of the system in terms of PEP. In general, an increase of the inertia is able to increase significantly the cooling energy production of the plant while a reduction of the inertia has a positive effect in terms of electrical energy production. Differently from the previous configurations, the effect of different temperature ranges at the HTT with inertia is limited despite reduced temperature ranges are still preferable.

With respect to the influence of the DNI, it has been evaluated considering a plant configuration operating with reduced temperature ranges at the HTT, a SM equal to 2 and an inertia as in the baseline configuration and located in the city of Palermo in Italy. Despite the limited difference in latitude between the city of Orte, where the prototype plant is located, and the city of Palermo the overall performance of the system increase of about 10% in terms of PEP compared to configuration C10. The system indeed is able to achieve almost 1600 h of operation in the city of Palermo with an electrical and cooling energy production triple compared to the baseline configuration C1 as reported in Figure 10.

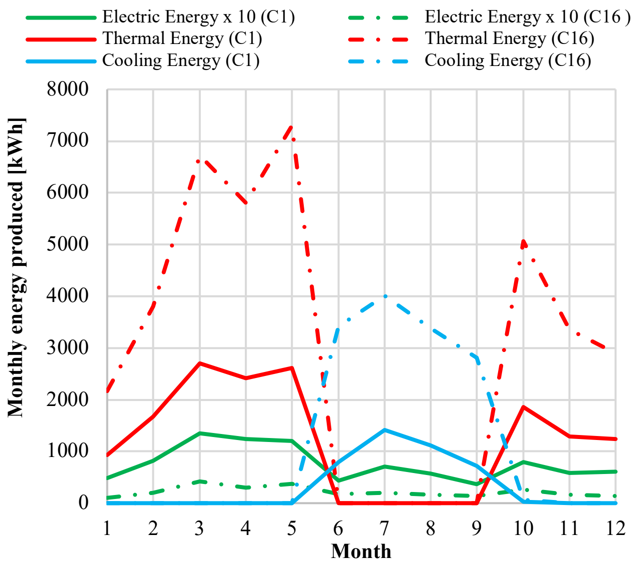

Figure 10 - monthly energy production of the trigeneration plant with city of Palermo DNI

Finally, Table 7 summarizes the annual average performance of the integrated system in the different configurations, including the $\eta_{glob,CCHP}$ given by the ratio between the sum of electric, thermal and cooling energy produced and the input solar energy at the CPC.

Table 7 – summary of annual average performance in the different configurations

Config.	η_{CPC} [%]	$T_{av,HTT}$ [°C]	$T_{av,LTT}$ [°C]	h_{ORC}	$\eta_{e,ORC}$ [%]	$\eta_{t,ORC}$ [%]	E_e [kWh]	E_t [kWh]	COP_{abs}	h_{abs}	E_c [kWh]	PEP [kWh]	$\eta_{glob,CCHP}$ [%]
C1	42.8	140.2	46.9	579.0	4.0	71.7	916.0	14713.9	0.647	256.4	4080.2	21191.5	22.4
C2	40.3	143.9	47.0	520.8	4.2	72.0	896.5	14102.8	0.647	209.9	3342.8	19947.9	20.9
C3	45.2	136.2	47.5	654.6	3.9	71.3	936.4	15061.1	0.648	340.6	5428.3	22576.8	24.4
C4	45.0	137.6	47.1	574.2	3.9	70.0	905.5	13455.6	0.647	371.5	5902.8	21063.6	23.1
C5	36.2	149.3	46.4	377.4	4.4	72.7	709.8	9633.3	0.647	251.3	3997.2	15048.8	16.3
C6	43.8	137.7	47.2	779.7	4.3	71.7	1045.5	14275.0	0.649	353.0	5670.0	22106.9	23.9
C7	34.4	148.0	46.2	524.2	4.7	71.9	864.6	10607.5	0.646	248.2	3945.8	16424.1	17.6
C8	45.0	136.2	47.6	1087.3	4.0	71.4	1631.0	24844.1	0.648	568.0	9052.1	37494.7	27.0
C9	39.7	142.6	47.2	840.6	4.3	71.9	1508.7	23538.9	0.647	323.9	5150.6	33017.2	22.9
C10	44.7	136.3	47.9	1457.3	4.2	71.5	2378.0	33738.9	0.647	784.7	12495.3	51409.1	27.7
C11	39.3	141.1	47.6	1151.8	4.5	72.0	2202.0	31880.6	0.647	499.0	7948.1	45744.9	23.9
C12	47.2	135.9	47.4	621.8	3.8	71.7	923.7	15439.9	0.647	401.6	6397.0	23657.6	25.9
C13	40.6	142.2	47.0	541.3	4.2	72.7	981.7	15678.7	0.647	261.5	4163.2	22462.1	23.7
C14	43.3	136.5	47.6	825.3	4.2	71.5	1064.3	15385.7	0.650	365.0	5838.7	23500.6	25.4
C15	39.1	143.7	47.0	654.5	4.6	72.1	1011.1	14661.1	0.647	222.2	3536.1	20949.3	21.9
C16	46.5	136.3	47.8	1585.8	4.2	71.6	2638.4	37119.8	0.6	862.1	13681.1	56560.7	29.3

The annual electric energy produced by the solar ORC CHP described by Calise et al. [17] in Naples is 4.3 MWh with a solar fraction of 95% and then it is 1.65 times bigger than the value of 2.6 MWh related to the 3 kWel unit of the present study. The difference is due to the area of solar collectors 1.47 times bigger (73.5 m^2 compared with 50 m^2), to a double electric peak power of the ORC unit (6 kW compared with 3 kW), to the 5% heat integration by an auxiliary heater and, especially, to the relevant heat fraction subtracted from the ORC to feed the absorption chiller. The different latitude, the use of flat plate collector compared with the CPC evacuated collectors and the ratio solar field area to nominal electric power of the ORC (12.25 m^2/kWe in [17] and 16.67 m^2/kWe in the present study) compensate in favour of the CCHP system here studied.

Finally, an economic analysis has been compared with results of the previous solar ORC-CHP study [17], considering the energy productivity of the CCHP ORC system represented in Table 7 and the maintenance cost estimated as a 1%/year of the overall system capital cost (733 €/year). The triple energy production, determined according to the basic configuration C3, amounts to 0.94 kWh_e, 15.06 MWh_t and 5.43 MWh_c respectively of electric, thermal and cooling energy. A cost of electric energy of 0.17 €/kWh_e and of natural gas of 0.80 €/Sm^3 [17] are reasonable values in Italy and have been used to determine the economic saving (avoided cost) generated by the solar ORC trigeneration system.

The exiguity of the yearly economic margin compared with the investment cost generates a Simple Pay Back unsatisfactory. Then, in spite of considering the contribution of incentive schemes represented by a 0.35 €/kWh_e feed-in-tariff for the net electricity produced and the Italian *Conto Termico,* introduced by Ministry for Economic Development and lately upgraded for solar cooling applications [40], amounting to a contribution of 12,600 €/year for 2 years, the Simple Pay Back of the investment is still unsatisfactory. An effective improvement of the investment could be reached only after the halving of the initial capital cost which would allow to determine a Pay Back of 13 years reached by Calise et al.[17] whose economic results were more cheering despite the consumption of natural gas requested by the auxiliary heater. A rise of the domestic energy costs would facilitate the mentioned improvement of the investment.

6. Conclusions

In this work, the performance of a prototype small scale concentrated solar ORC plant coupled with an absorption chiller has been evaluated during a whole year by means of TRNSYS. In general, the limited area of the collectors reduces the operating hours of the system and the electric energy production. On the contrary, the thermal efficiency of the ORC is high throughout the year and the resulting thermal and cooling energy production significant. Therefore, parametric analysis has been carried out in order to assess more efficient configurations of the system.

Effects on system performance of variation of working temperature ranges at the HTT, capacity of thermal tanks, fluid flow rates in the loops, solar multiple have been examined. The working temperature ranges at the HTT operating parameter has entailed the most relevant impact on the system overall performance. In particular, reduced temperature ranges allow to extend the operation of the trigeneration system throughout the year and to increase the primary energy production of about 6.5% compared to the baseline configuration. On the contrary, changes to fluid flow rates have negligible or negative effects on the system performance.

Later on, some selected design parameters have been also varied to evaluate potential rooms of improvement of the prototype plant. As regards the SM, simulations have shown that an increase of the SM has a positive effect on the operating hours of the plant, the ORC electric efficiency and the overall energy production: this effect is amplified by the choice of the reduced working temperature ranges. Nevertheless, the hours of operation of the integrated system still remain limited during the cold season because of the poor solar irradiation for the city of Orte.

Moreover, influence of the inertia of the system has been evaluated. Despite higher conversion efficiency of the CPC technology, an increase of the inertia of the system has a limited effect on the performance of the plant with the exception of the absorption chiller operating hours and cooling energy production. On the contrary, reducing the inertia of the system allows to increase the operating hours of the ORC unit and its electrical energy production compared to the baseline configuration. However, changing the inertia of the system has a minor effect on the overall performance of the system. Finally, influence of the DNI has been assessed considering a plant configuration operating with reduced temperature ranges at the HTT, a SM equal to 2 and an inertia as in the baseline configuration in the city of Palermo. Results have shown that higher solar irradiation can extend significantly the overall energy production of the plant and counterbalance the higher complexity of the system. In general, results here presented especially emphasize the importance of criteria concerning the operation of the plant, improvement of crucial system parameters control strategy and their effects. Indeed, the proper choice of operating parameters can improve the system performances with no additional costs and can furthermore amplify the benefits of ameliorative constructive parameters as the increase of the solar field area.

Therefore, in the near future, experimental tests of the prototype plant will be carried out with the final aim of comparing and potentially validating the presented simulation analysis. Future efforts will be put also in coupling the system with different energy user profiles in order to evaluate the dynamic performance of the integrated system according to different energy demand. Finally, the potential of an advanced control system able to adapt the system behavior to changing input conditions will be investigated in a subsequent phase.

Nevertheless, the economic analysis showed that the capital cost reduction is crucial and the installation of this system in high solar irradiation area, if possible on stand alone applications, is fundamental to assure a continuous operation throughout the year and to justify its higher complexity compared to traditional solar plants.

Acknowledgements

We thank The Ministry of the Environment and Protection of Land and Sea of Italy which between 2011 and 2013 funded the 24 months research project *STS – Solar Trigeneration System* from which started this activity regarding optimization of solar CCHP.

References

[1] Kristin Seyboth, Sverrisson F, Appavou F, Brown A, Epp B, Leidreiter A, et al. Renewables 2016 Global Status Report. 2016. doi:ISBN 978-3-9818107-0-7.

[2] IEA. Technology Roadmap Solar Thermal Electricity. 2014. doi:10.1007/SpringerReference_7300.

[3] Barlev D, Vidu R, Stroeve P. Innovation in concentrated solar power. Sol Energy Mater Sol Cells 2011;95:2703–25. doi:10.1016/j.solmat.2011.05.020.

[4] Santos-González I, García-Valladares O, Ortega N, Gómez VH. Numerical modeling and experimental analysis of the thermal performance of a Compound Parabolic Concentrator. Appl Therm Eng 2017;114:1152–60. doi:10.1016/j.applthermaleng.2016.10.100.

[5] Pei G, Li J, Ji J. Analysis of low temperature solar thermal electric generation using regenerative Organic Rankine Cycle. Appl Therm Eng 2010;30:998–1004. doi:10.1016/j.applthermaleng.2010.01.011.

[6] Wang J, Yan Z, Zhao P, Dai Y. Off-design performance analysis of a solar-powered organic Rankine cycle. Energy Convers Manag 2014;80:150–7. doi:10.1016/j.enconman.2014.01.032.

[7] Antonelli M, Baccioli A, Francesconi M, Desideri U, Martorano L. Electrical production of a small size Concentrated Solar Power plant with compound parabolic collectors. Renew Energy 2015;83:1110–8. doi:10.1016/j.renene.2015.03.033.

[8] Tchanche BF, Lambrinos G, Frangoudakis A, Papadakis G. Low-grade heat conversion into power using organic Rankine cycles – A review of various applications. Renew Sustain Energy Rev 2011;15:3963–79. doi:10.1016/j.rser.2011.07.024.

[9] Villarini M, Bocci E, Moneti M, Di Carlo A, Micangeli A. State of Art of Small Scale Solar Powered ORC Systems: A Review of the Different Typologies and Technology Perspectives. Energy Procedia 2014;45:257–67. doi:10.1016/j.egypro.2014.01.028.

[10] Li L, Ge YT, Luo X, Tassou SA. Experimental investigations into power generation with low grade waste heat and R245fa Organic Rankine Cycles (ORCs). Appl Therm Eng 2017;115:815–24. doi:10.1016/j.applthermaleng.2017.01.024.

[11] Al Jubori A, Daabo A, Al-Dadah RK, Mahmoud S, Ennil AB. Development of micro-scale axial and radial turbines for low-temperature heat source driven organic Rankine cycle. Energy Convers Manag 2016;130:141–55. doi:10.1016/j.enconman.2016.10.043.

[12] Pei G, Li J, Li Y, Wang D, Ji J. Construction and dynamic test of a small-scale organic rankine cycle. Energy 2011;36:3215–23. doi:10.1016/j.energy.2011.03.010.

[13] Li J, Pei G, Li Y, Wang D, Ji J. Energetic and exergetic investigation of an organic Rankine cycle at different heat source temperatures. Energy 2012;38:85–95.

doi:10.1016/j.energy.2011.12.032.
[14] Quoilin S, Orosz M, Hemond H, Lemort V. Performance and design optimization of a low-cost solar organic Rankine cycle for remote power generation. Sol Energy 2011;85:955–66. doi:10.1016/j.solener.2011.02.010.
[15] He Y-L, Mei D-H, Tao W-Q, Yang W-W, Liu H-L. Simulation of the parabolic trough solar energy generation system with Organic Rankine Cycle. Appl Energy 2012;97:630–41. doi:10.1016/j.apenergy.2012.02.047.
[16] Borunda M, Jaramillo OA, Dorantes R, Reyes A. Organic Rankine Cycle coupling with a Parabolic Trough Solar Power Plant for cogeneration and industrial processes. Renew Energy 2016;86:651–63. doi:10.1016/j.renene.2015.08.041.
[17] Calise F, d'Accadia MD, Vicidomini M, Scarpellino M. Design and simulation of a prototype of a small-scale solar CHP system based on evacuated flat-plate solar collectors and Organic Rankine Cycle. Energy Convers Manag 2015;90:347–63. doi:10.1016/j.enconman.2014.11.014.
[18] Comodi G, Cioccolanti L, Renzi M. Modelling the Italian household sector at the municipal scale: Micro-CHP, renewables and energy efficiency. Energy 2014;68:92–103. doi:10.1016/j.energy.2014.02.055.
[19] Rosato A, Sibilio S, Scorpio M. Dynamic performance assessment of a residential building-integrated cogeneration system under different boundary conditions. Part I: Energy analysis. Energy Convers Manag 2014;79:731–48. doi:10.1016/j.enconman.2013.10.001.
[20] Caliano M, Bianco N, Graditi G, Mongibello L. Economic optimization of a residential micro-CHP system considering different operation strategies. Appl Therm Eng 2016;101:592–600. doi:10.1016/j.applthermaleng.2015.11.024.
[21] Angrisani G, Roselli C, Sasso M, Tariello F. Dynamic performance assessment of a micro-trigeneration system with a desiccant-based air handling unit in Southern Italy climatic conditions. Energy Convers Manag 2014;80:188–201. doi:10.1016/j.enconman.2014.01.028.
[22] Chang H, Wan Z, Zheng Y, Chen X, Shu S, Tu Z, et al. Energy analysis of a hybrid PEMFC–solar energy residential micro-CCHP system combined with an organic Rankine cycle and vapor compression cycle. Energy Convers Manag 2017;142:374–84. doi:10.1016/j.enconman.2017.03.057.
[23] Boyaghchi FA, Heidarnejad P. Thermoeconomic assessment and multi objective optimization of a solar micro CCHP based on Organic Rankine Cycle for domestic application. Energy Convers Manag 2015;97:224–34. doi:10.1016/j.enconman.2015.03.036.
[24] Bocci E, Villarini M, Vecchione L, Sbordone D, Di Carlo A, Dell'Era A. Energy and Economic Analysis of a Residential Solar Organic Rankine Plant. Energy Procedia 2015;81:558–68. doi:10.1016/j.egypro.2015.12.135.
[25] Tuscia University. STS Solar Trigeneration System - Research Project. Viterbo: 2013.
[26] Kloben Industries srl n.d. http://en.kloben.it/ (accessed August 28, 2017).
[27] Newcomen n.d. http://i-greenenergy.it (accessed September 29, 2017).
[28] Maya Yazaki Europe Distributor n.d. www.maya-airconditioning.com/ (accessed August 28, 2017).
[29] Therminol ® 62 Heat Transfer Fluid n.d. http://www.therminol.com/products/Therminol-62 (accessed August 28, 2017).
[30] Enertecna srl. Enertecna srl Engineering Company. 2017 n.d. http://www.enertecna.com/index.html (accessed February 2, 2018).
[31] TRNSYS – Transient System Simulation Tool n.d. http://www.trnsys.com/ (accessed August 28, 2017).
[32] Matlab Mathworks n.d. https://www.mathworks.com/products/matlab.html (accessed August 28, 2017).
[33] Coolprop n.d. http://www.coolprop.org (accessed August 28, 2017).
[34] Decree 412/93 1993. http://www.gazzettaufficiale.it/eli/id/1993/10/14/093G0451/sg

(accessed September 29, 2017).
[35] Bianchi M, Branchini L, De Pascale A, Orlandini V, Ottaviano S, Pinelli M, et al. Experimental Performance of a Micro-ORC Energy System for Low Grade Heat Recovery. Energy Procedia 2017;129:899–906. doi:10.1016/J.EGYPRO.2017.09.096.
[36] Bianchi M, Branchini L, De Pascale A, Orlandini V, Ottaviano S, Peretto A, et al. Experimental Investigation with Steady-State Detection in a Micro-ORC Test Bench. Energy Procedia 2017;126:469–76. doi:10.1016/J.EGYPRO.2017.08.222.
[37] Scott K, Daly H, Barrett J, Strachan N. National climate policy implications of mitigating embodied energy system emissions. Clim Change 2016;136:325–38. doi:10.1007/s10584-016-1618-0.
[38] AEEG. AEEG Resolution EEN 3/08. 01 April 2008 2008. https://www.autorita.energia.it/it/docs/08/003-08een.htm (accessed October 18, 2017).
[39] Lubis A, Jeong J, Saito K, Giannetti N, Yabase H, Idrus Alhamid M, et al. Solar-assisted single-double-effect absorption chiller for use in Asian tropical climates. Renew Energy 2016;99:825–35. doi:10.1016/j.renene.2016.07.055.
[40] Ministry for Economic Development. Decree of Italian Ministry for Economic Development 16 February 2016 n.d. http://www.sviluppoeconomico.gov.it/images/stories/normativa/allegato_decreto_interministeriale_16_febbraio_2016_aggiornamento_conto_termico.pdf (accessed February 3, 2018).